Fibrin phantom for use in optical coherence tomography

Brendan F. Kennedy,[a,*] Susanne Loitsch,[a] Robert A. McLaughlin,[a] Loretta Scolaro,[a] Paul Rigby,[b] and David D. Sampson[a,b]

[a]The University of Western Australia, Optical+Biomedical Engineering Laboratory, School of Electrical, Electronic and Computer Engineering, 35 Stirling Highway, Crawley, Western Australia 6009, Australia
[b]The University of Western Australia, Centre for Microscopy, Characterisation and Analysis, 35 Stirling Highway, Crawley, Western Australia, 6009, Australia

Abstract. This work presents a novel tissue-mimicking phantom for use in a range of optical coherence tomography (OCT) experiments. Such phantoms are critical in the development and assessment of new OCT techniques, but no previously published phantoms have become universally accepted. We present the first description of a phantom based on a fibrin matrix, which improves key attributes of previously published methods. It provides a biocompatible, optically transparent scaffold in which to incorporate organic and/or inorganic optical scattering materials. Its fabrication time is markedly shorter than many common phantoms, and its lifetime is longer than other biocompatible phantoms. The potential of fibrin phantoms incorporating Intralipid™ to introduce uniform optical scattering is demonstrated. The measured attenuation coefficient as a function of Intralipid concentration confirms the ability to control optical scattering. A bilayer phantom with distinct optical scattering in each layer is also presented. [DOI: 10.1117/1.3427249]

Keywords: Fibrin; optical coherence tomography; tissue-mimicking phantom.

Paper 09568LRR received Dec. 22, 2009; revised manuscript received Mar. 15, 2010; accepted for publication Apr. 12, 2010; published online May 10, 2010.

1 Introduction

An important aspect of research in optical coherence tomography (OCT) is the validation of new systems, novel techniques, and theoretical predictions using phantoms with optical properties that closely approximate those of tissue.[1] Numerous such phantoms have been proposed;[1–3] however, issues exist with each of these phantoms and no previously published phantom has become universally accepted within the OCT community. OCT phantoms generally comprise a bulk matrix, which provides a scaffold, and additives, which provide optical absorption and scattering. For many experiments, it is important to use a matrix that allows for the incorporation of the natural constituents of tissue, such as blood and fat, to closely approximate tissue optical properties.[1]

Room-temperature vulcanizing (RTV) silicone, epoxy resin, and polyvinyl alcohol (PVA) gels are commonly used matrix materials.[1–3] However, these materials are not compatible with biological materials; therefore, inorganic scatterers must be used, typically white metal-oxide powders or microspheres. White metal-oxide powders, such as aluminum oxide (Al_2O_3) and titanium dioxide (TiO_2), have the disadvantage that their refractive index is much higher than that of tissue, resulting in phantoms with overall optical properties very different to those of tissue. An alternative is the more expensive dry silica microspheres, which have low size variations and a refractive index closer to tissue. However, it is difficult to achieve homogenously scattering phantoms with these particles due to aggregation.[2] For PVA gels, scattering is deliberately introduced into the matrix material by performing a series of freeze/thaw cycles.[3] However, PVA gels are not biologically compatible. Phantoms based on biologically compatible gelatin and agarose hydrogels have been used as phantom materials.[1] Scattering from the gelatin matrix has been reported, which is undesirable as it limits the degree to which scattering is controlled by additive concentration. Such gelatin and agarose phantoms typically have short lifetimes of less than one week, and do not maintain their rigidity at room temperature.[1]

In this work, we present novel, biocompatible phantoms based on a low-scattering matrix material that improves key attributes associated with commonly used phantom materials, including time-efficient fabrication, longer lifetime, rigidity at room temperature, and low scattering. We define biocompatible as a material that is suitable for the addition of biological materials and substances such as the constituents of tissue. The matrix material used is fibrin, which is employed as an adhesive in surgical procedures and wound closures.[4,5] Fibrin is a naturally occurring protein in humans that provides structural support for blood clots. It is formed from the protein fibrinogen by proteolysis induced by the enzyme thrombin. To demonstrate fibrin's potential, we used it to fabricate phantoms with optical scattering coefficients similar to those of tissue by incorporating it with Intralipid™. The main advantages of Intralipid are its well-known optical properties[6] and the similarity of its microparticles to lipid cell membranes and organelles that constitute the scattering sources in tissue.[1] The result is a homogeneous, uniformly scattering phantom, with a scattering coefficient that can be controlled by the concentration of Intralipid. Single and bilayer phantoms were fabricated and imaged using OCT. This paper provides the first description of fibrin-based OCT phantoms, detailing both fabrication techniques and the resulting optical properties.

2 Methods

Fibrin phantoms were fabricated using a mixture of fibrinogen and thrombin, both extracted from bovine plasma (Sigma-Aldrich, Germany). A quantity of 0.8 mg of thrombin powder was dissolved in 1 ml of saline, to which 40 μmol of calcium chloride ($CaCl_2$) was added. $CaCl_2$ reduces the clotting time and increases the elasticity of fibrin gels.[4] Separately, 70 mg of fibrinogen powder (65% to 85% protein) was dissolved in

*Address all correspondence to: Brendan F. Kennedy, The University of Western Australia, Optical+Biomedical Engineering Laboratory, School of Electrical, Electronic and Computer Engineering, 35 Stirling Highway, Crawley, Western Australia 6009, Australia. Tel: 006186-488-4746; Fax: 006186-488-1319; E-mail: brendank@ee.uwa.edu.au

1083-3668/2010/15(3)/030507/3/$25.00 © 2010 SPIE

1 ml of saline and mixed with a suitable volume of standard 20% Intralipid, where 20% signifies the percentage weight per volume (w/v) of soy bean oil. A 500-ml volume of 20% Intralipid contained 100 g of soybean oil, 6 g of egg lecithin, 11 g of glycerol, and water. The fibrinogen/Intralipid and thrombin/$CaCl_2$ solutions were mixed in a 3:2 volume ratio. The solution was set in a cylindrical mold of diameter 10 mm and thickness 3 mm. After 10-min clotting time, the fibrin phantom was placed in saline and stored in the refrigerator. This procedure resulted in a homogeneous distribution of optical scatterers, without observable aggregation. Bilayer phantoms were fabricated by pouring fibrin into the base of the mold in two steps. By controlling the volume of solution added to the mold, a thin layer (with 1% w/v Intralipid) was fabricated, followed by a thicker layer (with 13% w/v Intralipid) added 10 min later.

3 Experiment

Scanning electron microscope (SEM) images of a single-layer fibrin phantom were obtained. To record the images, a 1-mm-thick section of fibrin phantom was prepared by freeze drying in liquid nitrogen, and a 6-nm platinum surface coating was applied. The magnification was 74 K× and the accelerating voltage was 5 kV. In addition, confocal fluorescence microscopy images of a similar phantom were obtained. The phantom was eosin stained for 10 min to introduce fluorescent optical contrast, then rinsed in water for 15 min and imaged at a magnification of 60×.

To quantify the attenuation coefficient μ_t in fibrin phantoms, we used the technique described in Ref. 7. The sample reflectance $R(z)$ measured from the OCT signal is proportional to the product of the confocal point-spread function (PSF) with the single-scattering model for light attenuation in tissue[7]:

$$R(z) \propto \frac{1}{(z - z_{cf}/z_R)^2 + 1} \exp(-2\mu_t z), \qquad (1)$$

where z represents physical path length, and $z=0$ corresponds to the sample interface, z_{cf} is the position of the confocal gate, z_R is the apparent Rayleigh length used to characterize the point-spread function (PSF), and μ_t represents the attenuation coefficient. The confocal PSF was measured experimentally by moving a reflector through the focus of the sample beam and recording the detector output. As $R(z)$ and the confocal PSF were measured experimentally, Eq. (1) could be used to extract μ_t from measured OCT A-scans.

The attenuation coefficient of fibrin phantoms was measured using a time-domain OCT (TD-OCT) system. A broadband source ($\lambda=1310$ nm, $\Delta\lambda=154$ nm, axial resolution 6.4 μm) with an optical power of 21 mW was employed. The theoretical lateral resolution was 11.2 μm.

3-D datasets (XYZ) were recorded with $512\times600\times2048$ pixels. The reflectance $R(z)$ was extracted from the OCT signal by calibration from a series of reflectance standards. To reduce the effect of speckle on the calculation of μ_t, regions of 20 pixels in the Y-Z plane were averaged. A swept-source OCT system (Thorlabs, Newton, New Jersey) was used to image the bilayer fibrin phantom. A broadband source

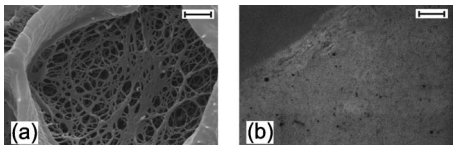

Fig. 1 (a) SEM image of fibrin matrix; scale bar represents 100 nm. (b) Confocal fluorescence microscope image of fibrin phantom containing Intralipid; scale bar represents 30 μm.

($\lambda=1300$ nm, $\Delta\lambda=100$ nm, axial resolution 12 μm) with an optical power of 10 mW was employed. The theoretical lateral resolution was 15 μm.

4 Results and Discussion

A scanning electron microscope image of a fibrin phantom, without Intralipid, is shown in Fig. 1(a). During the clotting process, the fibrin fibers aggregate and branch to form a 3-D matrix. This fibrous structure is shown in Fig. 1(a). The nanoscale of the structure results in a sufficiently low optical scattering cross section for the phantom to be optically transparent at wavelengths used for OCT. Figure 1(b) shows a confocal fluorescence microscope image of a fibrin phantom prepared with 19% w/v Intralipid. Fig. 1(b) shows the homogeneous nature of the fluorescence. The air-phantom interface is visible in the top-left. The dark, largely circular features present throughout the image and ranging in size from 0.5 to 5 μm are believed to be lipid droplets, which appear dark due to the absence of eosin.

The measured values of μ_t for phantoms with varying concentrations of Intralipid are presented in Fig. 2. For each concentration, measurements were recorded at intervals of 600 μm and averaged. The error bars represent one standard deviation (SD), calculated from five data points. A monotonic increase in scattering was measured for increasing Intralipid concentration. The values of μ_t presented in Fig. 2 are within the range of previously measured values for both tissue[8] and Intralipid.[6] In the inset of Fig. 2, the reflectance is plotted as a function of z. The slope (red line) is proportional to μ_t. The gradual increase in reflectance over the first 50 μm is attributed to diffusion of index-matching glycerol into the phantom near the boundary. The measured values of μ_t were stable for

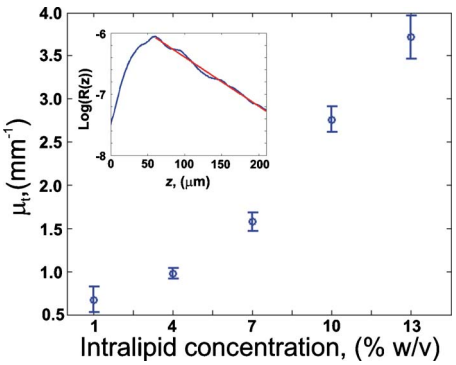

Fig. 2 Attenuation coefficient μ_t measured for phantoms with different % w/v concentrations of Intralipid. The inset shows the log-averaged OCT reflectance versus z, and the linear fit of attenuation (red line) for a phantom with 13% Intralipid. (Color online only.)

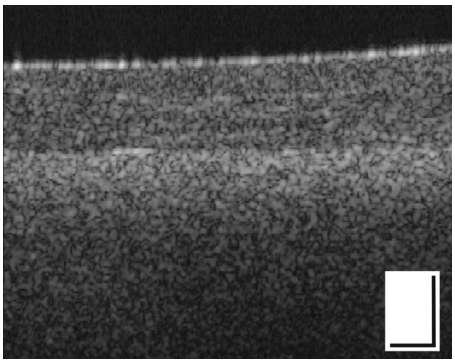

Fig. 3 Bilayer fibrin phantom, with different Intralipid concentration in both layers. The scale bar represents dimensions 300×300 μm.

a period of approximately two weeks. After this, leaching of the Intralipid resulted in a reduction in μ_t. However, the fibrin matrix remained intact for more than one month.

An OCT B-scan of a bilayer fibrin phantom is presented in Fig. 3. Higher scattering in the thicker layer is visible. The values of μ_t measured using the TD-OCT system in the thin and thick layers were 1.7 mm^{-1}, SD 0.1 mm^{-1}, and 3.3 mm^{-1}, SD 0.2 mm^{-1}, respectively. Comparing these values with Fig. 2, μ_t in the thin layer (Intralipid concentration 1%) is higher than expected, while μ_t in the thick layer (Intralipid concentration 13%) is lower than expected. We speculate that these differences are due to leaching of Intralipid from the thick layer to the thin layer during fabrication. This leaching could potentially be reduced by fabricating the phantoms at lower temperature. We subsequently observed a constant μ_t from both layers over a two-week period. We verified the integrity of the phantom over time by visual inspection. The homogeneity of each layer is visible in Fig. 3. The small inhomogeneities visible in the first layer are caused by small variations in Intralipid concentration resulting from imperfect mixing. The interface between layers is located at a depth in optical path length of approximately 370 μm.

The fibrin phantoms presented in this work are suitable for use in a wide range of experiments in OCT. The fabrication time for the phantom was approximately 30 min. In comparison, bilayer silicone phantoms fabricated in our laboratory require up to 24-h fabrication time.[9] The demonstrated homogeneity of fibrin phantoms will be important, for example, in studies of speckle in OCT, and measurement and use of the OCT scattering coefficient.[7,10] Investigations of the scattering properties of tissue constituents could be performed, and is the subject of ongoing work. Fibrin phantoms have the further advantage that they are pliable and exhibit a viscoelastic response that is in the range of biological tissues. It has been reported that the elastic modulus of fibrin can be changed by varying the thrombin concentration.[5] Thus, fibrin phantoms could be useful in OCT elastography studies.[9,11] It has further been reported that the viscosity of fibrin can be varied by increasing the fibrinogen concentration,[5] potentially mimicking the viscous properties of tissue. The ability to match a phantom's mechanical properties to those of tissue is important for interstitial OCT measurements and/or procedures in solid tissues.[12] Tumor-mimicking features can readily be incorporated into the fibrin matrix for such experiments.

5 Conclusions

Novel fibrin-based tissue-mimicking phantoms for use in OCT are presented. Fibrin phantoms overcome problems that exist in other biocompatible phantoms, such as scattering from the matrix, loss of rigidity at room temperature, and a short lifetime, and have a shorter fabrication time than commonly used phantoms. The fibrin matrix is optically transparent and compatible with both organic and inorganic optical scatterers. We demonstrate that fibrin phantoms incorporating Intralipid are homogeneous, provide controllable optical attenuation, and can readily be fabricated into two layers with distinct optical properties. These phantoms are well suited to a range of OCT experiments, in particular, those requiring homogeneous scattering, the addition of biological scatterers, and potentially those requiring viscoelastic properties matched to those of tissue. Fibrin phantoms have the potential to be adopted in a wide range of OCT applications.

Acknowledgments

The authors acknowledge the facilities, and scientific and technical assistance (in particular Peter Duncan) of the Australian Microscopy and Microanalysis Research Facility at the Centre for Microscopy, Characterisation and Analysis, The University of Western Australia, a facility funded by The University, State, and Commonwealth Governments.

References

1. B. W. Pogue and M. S. Patterson, "Review of tissue simulating phantoms for optical spectroscopy, imaging and dosimetry," *J. Biomed. Opt.* **11**(4), 041102 (2006).
2. C. E. Bisaillon, G. Lamouche, R. Maciejko, M. Dufour, and J. P. Monchalin, "Deformable and durable phantoms with controlled density of scatterers," *Phys. Med. Biol.* **53**, 237–247 (2008).
3. C. U. Devi, R. M. Vasu, and A. K. Sood, "Design, fabrication, and characterization of a tissue-equivalent phantom for optical elastography," *J. Biomed. Opt.* **10**(4), 1–10 (2005).
4. D. S. Feldman, and D. H. Sierra, "Tissue adhesives in wound healing," Chap. 40 in *Encyclopedic Handbook of Biomaterials and Bioengineering, Part A: Materials*, D. L. Wise, D. J. Trantolo, D. E. Altobelli, M. J. Yaszemski, J. D. Gresser, and E. R. Schwartz, Eds., pp. 1347–1384, Marcel Dekker, New York (1995).
5. H. Kaetsu, T. Uchida, and N. Shinya, "Increased effectiveness of fibrin sealant with a higher fibrin concentration," *Int. J. Adhes. Adhes.* **20**, 27–31 (2000).
6. H. J. van Staveren, C. J. M. Moes, J. van Marle, S. A. Prahl, and M. J. C. van Gemert, "Light scattering in intralipid-10% in the wavelength range of 400–1100 nm," *Appl. Opt.* **30**(31), 4507–4514 (1991).
7. D. J. Faber, F. J. Van der Meer, and M. C. G. Aalders, "Quantitative measurements of attenuation coefficients of weakly scattering media using optical coherence tomography," *Opt. Express* **12**(19), 4353–4365 (2004).
8. V. Tuchin, *Tissue Optics: Light Scattering Methods and Instruments for Medical Diagnosis*, SPIE Press, Bellingham, WA (2007).
9. B. F. Kennedy, T. R. Hillman, R. A. McLaughlin, B. C. Quirk, and D. D. Sampson, "*In vivo* dynamic optical coherence elastography using a ring actuator," *Opt. Express* **17**(24), 21762–21772 (2009).
10. R. A. McLaughlin, L. Scolaro, P. Robbins, C. Saunders, S. L. Jacques, and D. D. Sampson, "Mapping tissue optical attenuation to identify cancer using optical coherence tomography," in *Proc. MICCAI*, *Lect. Notes Comput. Sci.* **5762**, 657–664 (2009).
11. J. M. Schmitt, "OCT elastography: imaging microscopic deformation and strain of tissue," *Opt. Express* **3**(6), 199–211 (1998).
12. X. Li, C. Chudoba, T. Ko, C. Pitris, and J. G. Fujimoto, "Imaging needle for optical coherence tomography," *Opt. Lett.* **25**(20), 1520–1522 (2000).